Chemically resolved dynamical imaging of catalytic reactions on composite surfaces

F. Esch [a], S. Günther [a], E. Schütz [b], A. Schaak [b], I.G. Kevrekidis [c], M. Marsi [a], M. Kiskinova [a] and R. Imbihl [b]

[a] *Sincrotrone Trieste, Area Science Park, 34012 Basovizza, Italy*
[b] *Institut für Physikalische Chemie und Elektrochemie, Universität Hannover, Callinstr. 3–3a, D-30167 Hannover, Germany*
[c] *Department of Chemical Engineering, Princeton University, Princeton, NJ 08544-5263, USA*

Received 11 December 1997; accepted 11 March 1998

The catalytic reduction of NO by hydrogen is investigated at $T = 650$ K and $p \approx 10^{-6}$ mbar on a microstructured Rh/Pt(100) surface consisting of Pt(100) domains surrounded by a 600 Å thick Rh film. Synchrotron radiation scanning photoemission microscopy (SPEM), using photons focused into a spot of less than 0.2 μm diameter, is employed as a spatially and chemically resolving *in situ* technique. The chemical waves which arise in the bistable system NO + H_2/Rh are imaged with SPEM monitoring the N 1s and O 1s photoelectrons. The reaction fronts initiate transitions from an inactive oxygen-covered surface ($\Theta_O \approx 0.25$ ML) to a reactive nitrogen-covered surface ($\Theta_N \approx 0.06$ ML). At the Pt/Rh interface, synergetic effects can be observed: the chemical waves on the Rh film nucleate preferentially at the Pt/Rh interface. This nucleation is poisoned by carbon contamination on the Pt area but is prevented in the vicinity of the Pt/Rh interface by the adjacent clean Rh film. No segregation of Pt to the surface was observed for the 600 Å thick Rh film.

Keywords: chemical waves, NO reduction, Rh, Pt, microstructured composite surfaces, dynamical imaging, scanning photoemission microscopy, SPEM, photoemission electron microscopy, PEEM

1. Introduction

Real catalysts typically contain several components which are combined in order to obtain a catalytic performance superior to that of the individual constituents [1–3]. In order to understand the synergetic effects, a method is desirable that allows monitoring the distribution of the various adsorbate species and substrate constituents under reaction conditions. The recent development of spatially resolved photoemission with an ultrabright synchrotron source made feasible chemically and time-resolved imaging during the catalytic reactions. This opens the opportunity, in addition to a static microcharacterisation of the catalyst, to investigate dynamical effects as well [4].

This letter presents chemically resolved imaging of catalytic reactions on a Pt/Rh composite surface constructed by microlithography. Such a composite surface can be considered as a model catalyst for the automotive catalytic converters, since the conventional three-way catalyst (TWC) contains, on a ceramic support, highly dispersed Pt to which Rh is added because of its higher efficiency in dissociating NO [5]. We studied the $O_2 + H_2$ reaction to H_2O and the $NO + H_2$ reaction to N_2 and H_2O on a microstructured Rh/Pt(100) surface under isothermal conditions at low pressures ($p < 10^{-5}$ mbar). The dynamical behaviour of each reaction system is well known from a large number of single-crystal studies conducted mostly under low pressure conditions ($p < 10^{-3}$ mbar) [6–8]. On microstructured Rh/Pt(100) surfaces, these reactions were studied before using photoemission electron microscopy (PEEM) which images the local work function variation caused by the adsorbates [9,10]. Chemical waves initiating transitions between a high- and a low-reactivity state of the surface have been found.

PEEM, however, provides only limited information about the chemical identity of the imaged species. Moreover, on composite surfaces, intermixing due to lateral or vertical diffusion of the metals can occur leading to laterally varying changes in the composition of the substrate. Here we demonstrate that chemical imaging by scanning photoemission microscopy can be employed to examine *in situ* the compositional differences in the catalyst substrate and in the adsorbate layer, and allows for following the local dynamics on a micron scale. Different adsorbate species can be identified under reaction conditions, chemical waves can be imaged and synergetic effects can be observed at the interface of the two metals, Pt and Rh.

2. Experimental

The experiments were performed with the scanning photoemission microscope (SPEM) at the ELETTRA light source. The microscope uses a photon-focusing optical system (combination of a Fresnel zone plate and an order-sorting aperture) which can demagnify the beam to a spot with a diameter of less than 0.2 μm. Specific information about the composition and electronic structure of the surface and interface is provided by the photoelectron (PE) spectra measured with a hemispherical (HS) electron analyser,

mounted at a grazing angle of 70° with respect to the X-ray beam and the surface normal. This geometry enhances the surface sensitivity of the microscope. Spatially resolved chemical images were obtained by tuning the analyser to collect photoelectrons emitted from a specific core level of the surface and adsorbate layer constituents and scanning the sample with respect to the focused beam (acquisition time was about 30 ms/pixel). A more detailed description of the ESCA microscopy beamline and SPEM set-up can be found in [11]. In the present study, we used 620 eV photons to monitor the specific core levels of all metal constituents and of all species that can be present in the adsorbate layer. The energy resolution used was $\geqslant$1 eV for images and $\leqslant$0.6 eV for spectra. The binding energies were calibrated by using the $3d_{5/2}$ peak of the clean Rh film (307.2 eV) as a reference. The oxygen coverages given in this paper were calibrated by the intensity of the background-corrected O 1s spectrum of the oxygen-saturated Rh film, assuming that the saturation coverage of oxygen for NO adsorption at 650 K is 0.25 ML, as in the case of stepped Rh(533) and Rh(111) [12,13]. Nitrogen and carbon coverages were evaluated on the basis of the O 1s calibration by using the tabulated cross-sections for O 1s, N 1s and C 1s in [14].

As a model catalyst, we used a Pt(100) single-crystal surface on which a thin Rh layer of 600 Å thickness had been deposited via a negative photoresist process. In this way, Pt domains of varying geometry and size were created, surrounded by a reactive Rh layer. Before introduction to the SPEM, Auger electron spectra taken after brief Ar ion sputtering showed the presence of carbon which was expected to be removed under reaction conditions.

3. Results and discussion

First, we will illustrate and discuss the removal of the thin graphitic layer which remained on the microstructured Rh/Pt(100) surface after sputtering. The oxidation of the carbon to CO and CO_2 under reaction conditions, and thus cleaning of the catalyst surfaces, is a process that readily occurs in exhaust gas converters [5]. In particular, we examined the evolution of the surface composition after exposing the carbon-contaminated catalyst to a $NO + H_2$ ambient ($p_{NO} = 8 \times 10^{-8}$ mbar and varying H_2 pressures) at 650 K.

Figure 1(a) shows SPEM images of a surface area centered on a Pt circle of 20 μm diameter surrounded by the deposited Rh film, after being treated under reaction conditions for two days. Only after this long period, the formation of chemical waves occurred on the Rh film. The images are taken with the HS electron analyser tuned to the Pt $4f_{7/2}$, Rh $3d_{5/2}$, C 1s and O 1s photoelectrons. The contrast in the images corresponds to intensity variations of the PE signal and can be used as a fingerprint for the different

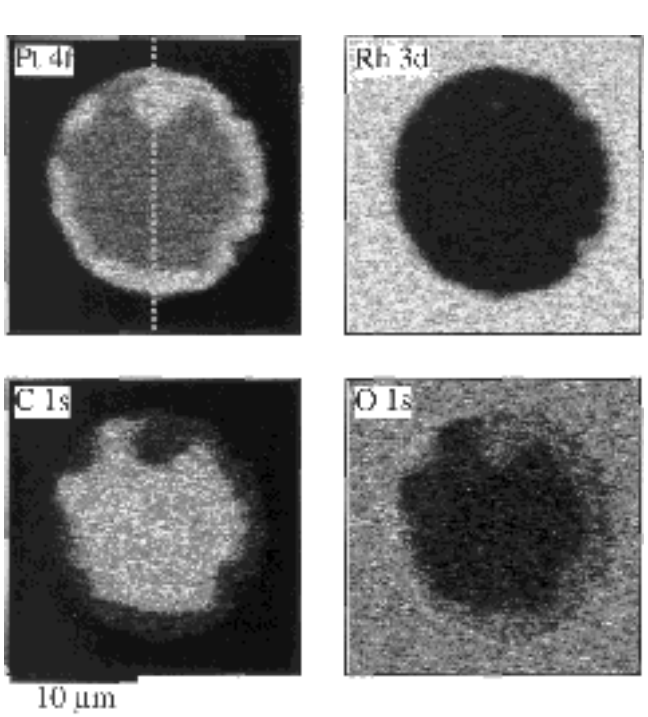

(a)

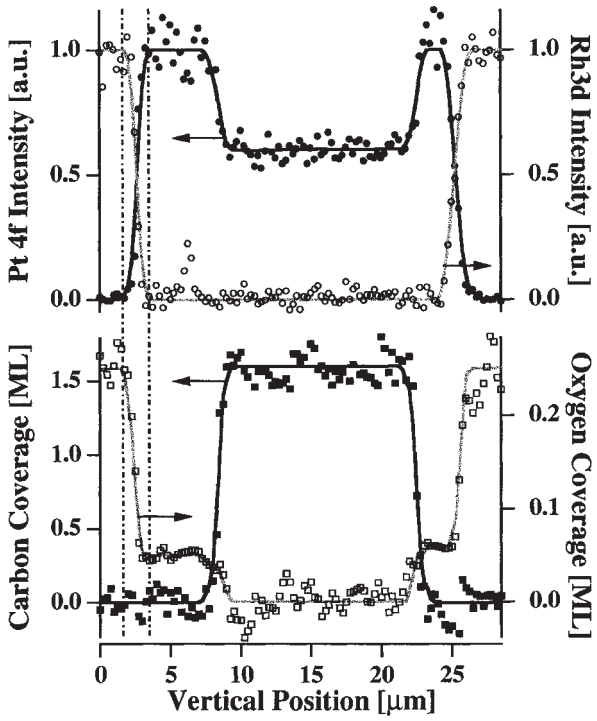

(b)

Figure 1. Reactive removal of a carbon layer on a microstructured Rh/Pt(100) catalyst. Experimental conditions: $p_{NO} = 8 \times 10^{-8}$ mbar and variable p_{H_2}, $T = 650$ K. (a) SPEM Pt $4f_{7/2}$, Rh $3d_{5/2}$, C 1s and O 1s images of a Pt circle surrounded by the Rh film taken after treatment of the catalyst for two days in an oxidizing $NO + H_2$ ambient. (b) Line profiles of the PE intensities obtained by a cut along the vertical dashed line marked in the Pt 4f image. The Pt 4f (filled circles) and the Rh 3d signal (open circles) are scaled to their respective maximum. The C 1s (filled squares) and the O 1s signal (open squares) are converted to coverages.

local concentrations of the elements on the surface and in the near-surface region. The Pt circle surrounded by the Rh film can be clearly seen in the Pt 4f and Rh 3d images. The C 1s image shows that, after a long treatment under $NO + H_2$ reaction conditions, the carbon film has been removed from the Rh surface and from the border areas of the Pt circle, but it is still present in the inner part of the Pt circle. The width of the carbon-free zone at the Pt border is 2–3 μm and is found to be the same for all microstructures on the surface; the larger carbon-free spot at the upper border of the Pt circle in the image series figure 1(a) is due to Rh remains on the Pt which can be distinguished as a brighter area in the Rh 3d image. The difference in the contrast of the carbon-clean Pt and Rh areas in the C 1s image is due to the different secondary background level on Pt and Rh and does not reflect different carbon coverages. This is consistent with the PE spectra taken from the different areas which confirmed that carbon can only be found inside the Pt circle where it reduces the Pt 4f signal by about 60%, as seen in the Pt 4f image.

The lateral changes in the concentration of Rh, Pt, carbon and oxygen are clearly manifested by the line profiles shown in figure 1(b), obtained by cutting the images in figure 1(a) on the line marked in the Pt 4f image. The Pt and Rh line profiles show that the pattern edge is rather sharp, i.e., the intermixing of the two metals is confined within less than 1 μm at the periphery. No Rh could be found inside the Pt circle, neither Pt on the Rh film. The C 1s and O 1s profiles show that in an oxidising ambient the carbon-free surface is covered by adsorbed oxygen. For these two species, we can convert the PE intensities to coverages, following the procedure described above. The obtained carbon coverage of 1.6 ML inside the Pt circle is in good agreement with the observed damping of the Pt 4f signal.

The presence of carbon only on Pt can tentatively be attributed to the different activity of Pt and Rh with respect to NO dissociation. On the Rh surface, the removal of the C layer via oxidation is faster because the NO dissociation which provides oxygen proceeds more effectively on Rh than on Pt. The efficient removal of C from the Pt edge areas in the vicinity of the Rh film indicates that the NO dissociation is also enhanced at the Pt/Rh interface region, consistent with the multiple edge effects exerted by laterally confined films (a 600 Å thick Rh film here) on the surrounding surface. Oxygen provided by NO dissociation on the Rh and at the rough Pt/Rh interface diffuses onto the Pt surface leading to propagation of the carbon oxidation front deeper into the Pt area. Similar cleaning of the carbon-contaminated Pt area was also observed on a sample with a thinner Rh film, where the cleaning could be followed until nearly complete carbon removal from the Pt area under $NO + H_2$ reaction.

The second aim of this study was to follow the dynamical changes in the adlayer composition related to the propagation of chemical waves formed during the $NO + H_2$ reaction on Rh. In this reaction system, which is bistable within the parameter range investigated here, reaction fronts initiate transitions between a non-reactive and a reactive state of the surface. Starting conditions are catalyst at temperature 650 K in a NO ambient ($p_{NO} = 8 \times 10^{-8}$ mbar), which lead to a saturation-oxygen coverage of $\approx$0.25 ML on the Rh surface. This oxygen-covered surface has low reactivity because the presence of oxygen inhibits dissociative adsorption of H_2 [8]. By introducing H_2 and increasing the p_{H_2} up to a sufficiently high value, a reaction front nucleates and reacts off the oxygen. This is accompanied by a build-up of an nitrogen layer, reaching a coverage of $\approx$0.06 ML.

The propagation of the reaction front is shown by the O 1s and N 1s images in figure 2, taken successively after introducing hydrogen in the gas phase ($p_{H_2} = 1.2 \times 10^{-7}$ mbar). Each N 1s image precedes the O 1s image. The dark triangle in the upper right corner is the Rh-free Pt substrate, the rest of the imaged area is the Rh film (the contrast between both metals is clearly visible in all images). In the lower right corner one can see an already propagating wave which has started from an interface below the imaged area. Nucleation and propagation of a new chemical wave, with a starting point marked by an arrow, can be seen in the second O 1s image. By cutting the O 1s and N 1s images in the lower part, as marked by the dashed line in the upper left image of figure 2(a), the line profiles of the chemical wave can be obtained. They are plotted in figure 2(b), after conversion of the PE intensities to coverages. In brief, the following important features should be noted from the images in figure 2: (i) the reaction front nucleates at the Pt/Rh interface (see the arrows in figure 2(a)); (ii) the propagating front causes a switching from an oxygen- to a nitrogen-covered surface; and (iii) the reduction of the hydrogen pressure reverses the propagation direction and restores the initial state.

The nucleation centers for these chemical waves are usually structural defects and/or areas with a different chemical composition on the surface [6]. The preferential nucleation of reaction fronts at the Pt/Rh interface is consistent with the properties of Pt, which has less affinity to oxygen than Rh [15]. Since the presence of oxygen inhibits H_2 dissociation, Pt preserves a certain activity for H_2 dissociation, because it adsorbs less oxygen. This explains the higher reactivity when both metals are in contact. The high reactivity of the Pt/Rh interface is also consistent with the enhanced catalytic activity found for the Pt/Rh alloys [15,16].

The present results clearly demonstrate that the chemical wave nucleates at the Pt/Rh interface and restores the active, reduced state of the Rh surface, if the interface is not carbon-contaminated. On the other hand, as described before, the C contamination of the interface is prevented by the adjacent Rh surface, thus providing an example for the synergistic effect of two components of a bimetallic catalyst under conditions which might model the cold start of a car-exhaust catalyst.

At the reaction front, the transition from the oxygen- to the nitrogen-covered Rh surface is rather sharp: the width of the N/O interface is less than 1 μm, as manifested by

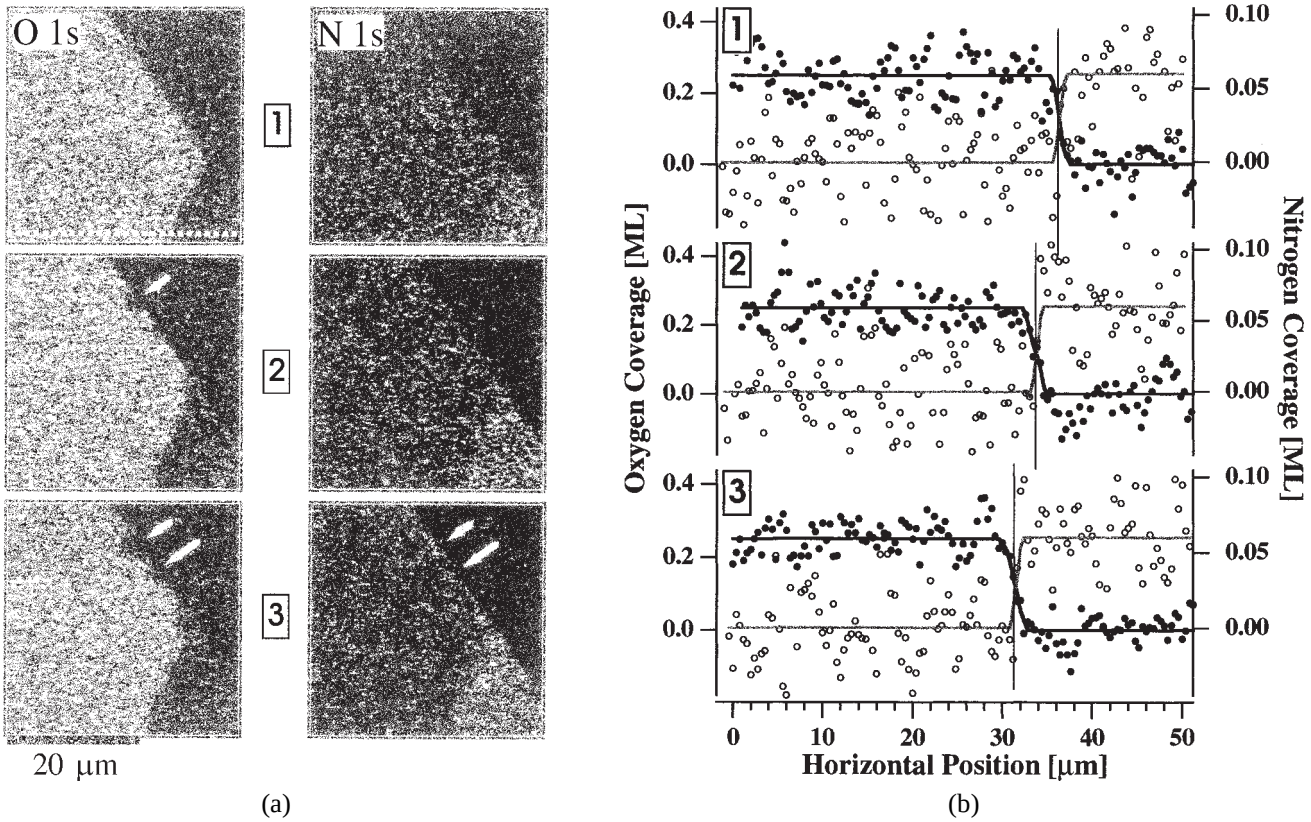

Figure 2. Propagation of a chemical wave during the $NO + H_2$ reaction on Rh after its nucleation at the Pt/Rh interface. Experimental conditions: $p_{NO} = 8 \times 10^{-8}$ mbar, $p_{H_2} = 1.2 \times 10^{-7}$ mbar, $T = 650$ K. Acquisition time per image 8 min. (a) SPEM images of oxygen, O 1s (left), and nitrogen, N 1s (right). The dark triangle in the upper right corner is the Rh-free Pt substrate, the rest of the imaged area is covered by the Rh film. The nucleation of a new chemical wave at the Pt/Rh interface, indicated by the arrow, and its propagation can be monitored (see text). (b) Line profiles showing the local coverages of oxygen (filled circles) and nitrogen (open circles) in the chemical wave. The profiles, obtained by a cut along the horizontal dashed line marked in the top O 1s image of figure 2(a), are converted to coverages.

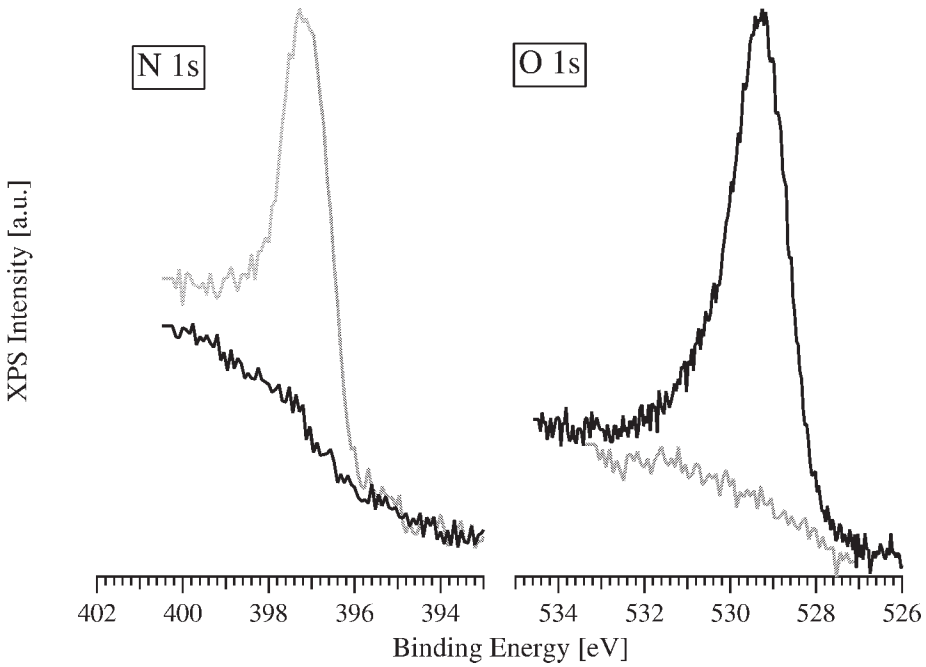

Figure 3. N 1s and O 1s XPS spectra recorded before (black line) and after passage of the reaction front (grey line) on the Rh film. The spectra indicate a complete switching from an oxygen to a nitrogen adlayer. Experimental conditions: $p_{NO} = 8 \times 10^{-8}$ mbar, $p_{H_2} = 1.2 \times 10^{-7}$ mbar, $T = 650$ K. The atomic nitrogen has a binding energy of 397.3 eV and the atomic oxygen of 529.5 eV.

the N 1s and O 1s line profiles in figure 2(b). It should be noted that the scatter in the N 1s data is due to the very low coverage of nitrogen, which correlates with the high catalytic activity and selectivity of Rh resulting in substantial thermal desorption of nitrogen at 650 K.

The PE spectra taken from different spots on the surface show that in the reaction system $NO + H_2$ only two surface species can be identified at $T = 650$ K, chemisorbed oxygen and chemisorbed nitrogen. Figure 3 demonstrates O 1s and N 1s spectra recorded from the Rh surface before and after passage of the reaction front. The presence of one species excludes always the presence of the other in the investigated parameter range. The binding energies (O 1s: 529.5 eV, and N 1s: 397.3 eV) are characteristic for chemisorbed oxygen and chemisorbed nitrogen species and correspond to binding energies measured on a stepped Rh(533) surface under similar conditions [12]. At $T = 650$ K, the dissociation of NH_x is already substantial on Rh surfaces and this should be the reason that no NH_x ($x = 1, 2$) species can be identified in the N 1s spectra [8]. A possible influence of photon-stimulated desorption cannot be ruled out, but the high photon flux ($\approx 10^9$ photons/s in the spot) does not modify the behaviour of the reaction, as compared with PEEM measurements conducted under the same conditions.

SPEM and PEEM measurements showed that the velocity of the reaction front can be tuned from stationary at $p_{H_2}/p_{NO} = 1$ up to 0.4 μm/s at $p_{H_2}/p_{NO} = 2$ (p_{NO} was kept constant). For p_{H_2}/p_{NO} less than 1, the direction of front propagation is reversed, indicating a true bistability of the reaction system. Comparable front velocities were also observed during the $O_2 + H_2$ reaction, demonstrating that chemisorbed nitrogen (at low coverages) has a negligible influence on the propagation of the reaction front.

Under the relatively mild reaction conditions of our experiments, no segregation of Pt to the surface of the Rh film was detected. In experiments under similar conditions, but with only a 70 Å thick Rh film on top of Pt(100), significant vertical intermixing occurred [17]. In the reversed system consisting of a 300 Å thick Pt film on top of Rh(110), oxygen-induced segregation of Rh to the Pt surface was observed [18]. The absence of detectable Pt segregation and surface alloying for the Rh film in our experiments can be attributed to (i) the large film thickness of 600 Å, and (ii) to the absence of a strong adsorbate-induced segregation, since the preferred binding partner of oxygen is Rh [15,16].

Pattern formation on microstructured surfaces was studied before for catalytic CO oxidation on Pt(110) and Pt(100) domains surrounded by an inert Ti/TiO_2 layer [19]. In these experiments, PEEM, used as a spatially resolved method, images the local work function, but yields no information about the chemical identity of the adsorbate. While such a shortcoming might be irrelevant for a chemically simple system as CO oxidation, for more complex systems the identification of the adsorbate species remains a challenging task. A number of other techniques based on a different contrast mechanism have also been applied to image chemical waves, such as low-energy electron microscopy (LEEM) [20], field electron (FEM) and field ion microscopy (FIM) [21], and optical methods [22]. Similar to PEEM, all these methods do not allow discrimination between different chemical species on the surface. Since a proper mechanistic understanding and realistic mathematical modelling require qualitative data about the surface species and quantitative data about the coverages, SPEM is a valuable tool for investigation of dynamical processes in catalysis.

4. Conclusion

In summary, this is the first photoemission microscopy study which shows that imaging of dynamical processes on catalytic surfaces with chemical contrast is possible. It has been demonstrated that the bistable $O_2 + H_2$ and $NO + H_2$ reactions on Rh exhibit transitions via reaction fronts between an inactive oxygen-covered state of the surface and an active reduced state (nitrogen-covered in the case of the $NO + H_2$ reaction).

On the bimetallic Pt/Rh model catalyst, we observe two synergetic effects at the Pt/Rh interface under reaction conditions: (i) Rh prevents poisoning of the adjacent Pt area by carbon contamination because it acts as a supplier for oxygen, and (ii) the Pt/Rh interface acts as a nucleation center for reaction fronts on the Rh which convert the surface to its reactive state. These two effects can be related to the fact that the catalytically more active Rh provides the oxygen for the reaction (via O_2 and NO dissociation) for both reactions: carbon oxidation and water formation. Pt, on the other hand, preserves a higher activity for H_2 dissociation and acts as a more active hydrogen source. The results of this study demonstrate in particular that the interface of two metals plays an important role when dynamical effects in catalytic reactions come into play.

Acknowledgement

We thank Diego Lonza for his excellent technical assistance. We acknowledge Dr. M. Gentili and his group from IESS for developing and providing the zone-plate optics. This work was financially supported by the BMBF (FRG), EC grant under contract no. EBRCH-GECT920013 and Sincrotrone Trieste SCpA.

References

[1] J.M. Thomas and W.J. Thomas, *Heterogeneous Catalysis* (VCH, Weinheim, 1996).
[2] J.H. Sinfelt, *Bimetallic Catalysts* (Wiley, New York, 1983).
[3] C.T. Campbell, Ann. Rev. Phys. Chem. 41 (1990) 775.
[4] M. Kiskinova and G. Paolucci, Surf. Sci. 377–379 (1997) 735.
[5] K.C. Taylor, in: *Automotive Catalytic Converters* (Springer, Berlin, 1984).
[6] R. Imbihl and G. Ertl, Chem. Rev. 95 (1995) 697.

[7] R.M. Wolf, J.W. Bakker and B.E. Nieuwenhuys, Surf. Sci. 246 (1991) 135.
[8] F. Mertens, S. Schwegmann and R. Imbihl, J. Chem. Phys. 106 (1997) 4319.
[9] E. Schütz, N. Hartmann, I.G. Kevrekidis and R. Imbihl, Faraday Disc. 105 (1996) 47.
[10] E. Schütz, N. Hartmann, I.G. Kevrekidis and R. Imbihl, Phys. Rev. Lett., submitted.
[11] M. Marsi, L. Casalis, L. Gregoratti, S. Günther, A. Kolmakov, J. Kovac, D. Lonza and M. Kiskinova, J. Electron Spectrosc. Rel. Phenom. 84 (1997) 73.
[12] P.D. Cobden, B.E. Nieuwenhuys, F. Esch, A. Baraldi, G. Comelli, S. Lizzit and M. Kiskinova, J. Vac. Sci. Technol., in press.
[13] H. Xu and K.Y.S. Ng, Surf. Sci. 375 (1997) 161.
[14] J.J. Yeh and I. Lindau, Atomic Data and Nuclear Data Tables 32 (1985) 1.
[15] A. Sasahara, H. Tamura and K.I. Tanaka, Catal. Lett. 28 (1994) 161; H. Tamura, A. Sasahara and K.I. Tanaka, Surf. Sci. 303 (1994) L379.
[16] H. Hirano, T. Yamada, K.I. Tanaka, J. Siera, P.D. Cobden and B.E. Nieuwenhuys, Surf. Sci. 262 (1992) 97.
[17] F. Esch, S. Günther, E. Schütz, A. Schaak, I.G. Kevrikidis, M. Marsi, M. Kiskinova and R. Imbihl, Surf. Sci., to be submitted.
[18] E. Schütz, F. Esch, S. Günther, A. Schaak, M. Marsi, M. Kiskinova and R. Imbihl, Science, submitted.
[19] M.D. Graham, I.G. Kevrekidis, K. Asakura, J. Lauterbach, K. Krischer, H.H. Rotermund and G. Ertl, Science 264 (1994) 80; M.D. Graham, M. Bär, I.G. Kevrekidis, K. Asakura, J. Lauterbach, H.H. Rotermund and G. Ertl, Phys. Rev. E 52 (1995) 76.
[20] S. Swiech, B. Rausenberger, W. Engel, A.M. Bradshaw and E. Zeitler, Surf. Sci. 294 (1993) 297.
[21] V. Gorodetskii, J.H. Block, W. Drachsel and M. Ehsasi, Appl. Surf. Sci. 67 (1993) 198; M.F.H. van Tol, A. Gielbert and B.E. Nieuwenhuys, Catal. Lett. 16 (1992) 297.
[22] H.H. Rotermund, G. Haas, R.U. Franz, R.M. Tromp and G. Ertl, Science 270 (1995) 608.